

## Chapter 2

# Structure and Imaging of a Transmission Electron Microscope (TEM)

In this chapter, we overview the structure of a transmission electron microscope (TEM) for nanoimaging, and mathematical descriptions of basic actions of a magnetic round lens are explained.

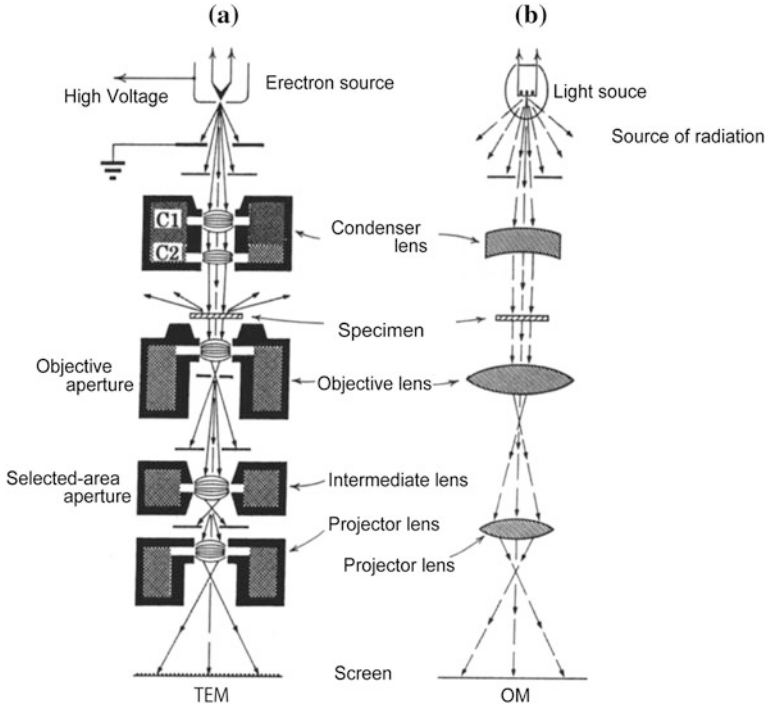
### 2.1 Structure of a Transmission Electron Microscope

Figure 2.1 shows a comparison of a transmission electron microscope (TEM) (a) with a light microscope (b). For easy comparison, a light source of the light microscope is located in an upper part of the instrument, which is a reversed arrangement from ordinary light microscopes, but the situation is adopted recently in many biological light microscopes. The light emitted from a light bulb or a laser is collimated by a condenser lens, where we can consider that a plane wave is illuminated onto a specimen. The exit waves from a backside of the specimen enter into an objective lens made of glass, and the image is formed at a distance from the lens as a reversed one. The image is transferred to a projector lens (or an eye-lens) to form the enlarged image.<sup>1</sup>

In an electron microscope, a similar thing happens apart from the existence of an intermediate lens, which changes the magnification of images and modes of imaging and diffraction. The well-known lens formula for a thin lens holds in the relation between the specimen (object) and the image. The total magnification is

---

<sup>1</sup>Optical parts including a lens have various kinds of aberrations, in which rays emitted from an object do not focus on the image plane. There are chromatic aberrations in which waves with different wavelength do not focus, and spherical aberration in which rays with large entrance angles do not converge. For optical microscopes, Seidel (1856) summarized five aberrations of a convex lens up to the third-order (see Born and Wolf 1970). Among them, the third-order spherical aberration limits the resolution of TEM since the invention of TEM in the beginning of the 1930s. Nowadays, the spherical aberration is almost corrected to give us the resolution of several tens picometer.



**Fig. 2.1** Comparison between a transmission electron microscope (TEM) (a) and an optical microscope (OM) (b)

$M = M_{\text{obj}} \times M_{\text{inter}} \times M_{\text{proj}}$ , where  $M_{\text{obj}}$  is magnification of the objective lens. It should be noted that the resolution is determined by aberrations of the objective lens as the first stage of an image forming system and the size of aperture of the lens. This is because the intermediate and projector lenses are used for enlargement<sup>2</sup> (Seidel 1856).

Without aberrations, the resolution of a microscope is given by Rayleigh's formula as

$$\delta = 0.61\lambda / \sin \alpha, \quad (2.1)$$

where  $\lambda$  is the wavelength of light or electron waves and  $\alpha$  is an acceptance angle of the objective lens, which is equal to the diffraction/scattering angles of waves by a specimen when it is located slightly outside from the front focal plane. This is a limitation of resolution due to the physical nature of light or electron waves.

<sup>2</sup>Blurred image by the first lens is still blurred after the second and third lenses for enlargement. The principle is discussed similarly to amplifiers for electrical signals. The signal/noise ratio is mainly determined by the first stage amplifier.

Recently, transmission electron microscopy using a scanning fine probe, that is STEM, is extensively developed. The details are described later in Chaps. 9 and 10 in this textbook. Hereafter, we see components of the TEM.

### Electron gun

A transmission electron microscope adopts the same configuration of lenses as that of a light microscope. The source of electrons works on a different physical phenomenon from that in a light microscope. We have several types of cathodes (electron emitters) such as a thermal cathode, a cold-field emission cathode, a thermal-field emission cathode, and a photocathode. In this section, we make a brief explanation of the cathodes for electron guns.

Let us start with a thermal cathode. The basic actions of the electron gun are (1) the electrofield extraction of electrons located near the Fermi level in heated source materials such as tungsten, lanthanum hexaboride ( $\text{LaB}_6$ ), and oxide-coated tungsten, by a few kV in applied voltage, and (2) focusing using electrostatic fields by the Wehnelt electrode (cap) to form the “crossover” below the electron gun, as illustrated in Fig. 2.2a. Figure 2.3 shows energy levels of electrons in metals on the left-hand side. On the right-hand side, the vacuum level outside the metals is described by a horizontal line (upper). The thermionic gun using a tungsten hairpin filament was developed in the beginning of the twentieth century and has been used in various kinds of instruments. The current density is given by Richardson-Dushman’s equation as follows:

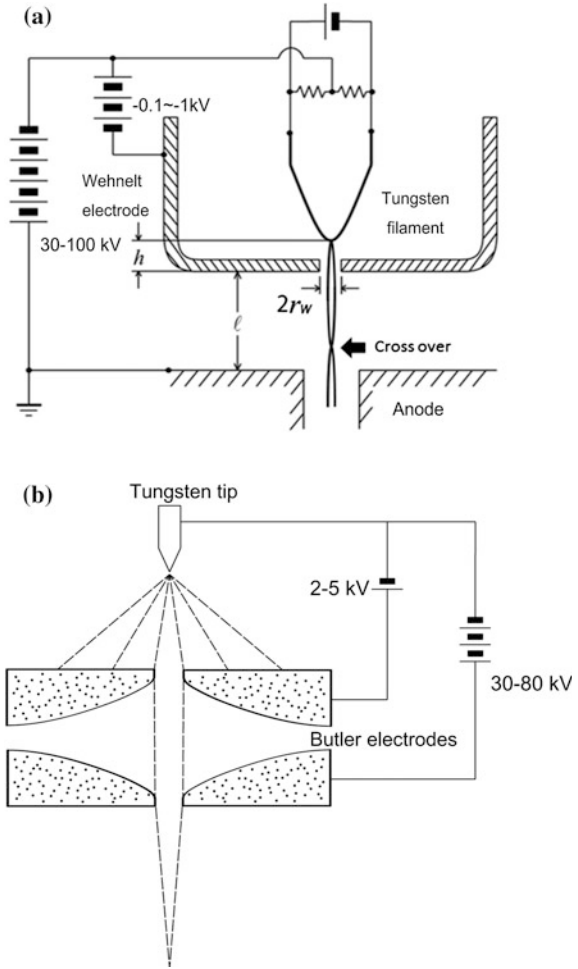
$$i = AT^2 \exp(-\phi_w/k_B T) \quad (2.2)$$

$$(A = 4\pi me k_B^2 h^{-3})$$

where  $\phi_w$  is the work function of a source material,  $k_B$  is the Boltzmann’s constant,  $m$  is the electron mass,  $e$  is the electron charge, and  $h$  is the Planck constant (Kittel 1966). The constant  $A$  amounts to  $120 \text{ A/cm}^2\text{deg}^2$ . The brightness is about  $10^5 \text{ A/cm}^2\text{sr}$ , which is enough for illumination of conventional TEM, but insufficient for high-resolution electron microscopy which necessitates higher magnification. Later, a pointed cathode (Hibi 1956) and a composite  $\text{LaB}_6$  cathode (Broers 1967) were developed. The brightness of the  $\text{LaB}_6$  cathode is about  $10^6 \text{ A/cm}^2\text{sr}$ . In the 1990s, these were intensively used for high-resolution TEM. However, STEM imaging at atomic resolution needs a higher brightness gun, that is, a field emission gun (FEG).

In the FEG in Fig. 2.2b, an extraction voltage of a few kV is applied to  $\langle 310 \rangle$  and  $\langle 100 \rangle$  oriented tungsten tips at ambient temperature or lower than 1300 K. The applied voltage narrows the width of the potential barrier at the metal surface smaller than that on the right-hand side of Fig. 2.3. An electron tunneling phenomenon then occurs, which is called “field emission.” Using Wentzel–Kramers–Brillouin (WKB) approximation (Schiff 1968), the current density is given by:

**Fig. 2.2** Basic structures of a thermionic gun (a) and a field emission gun (b)

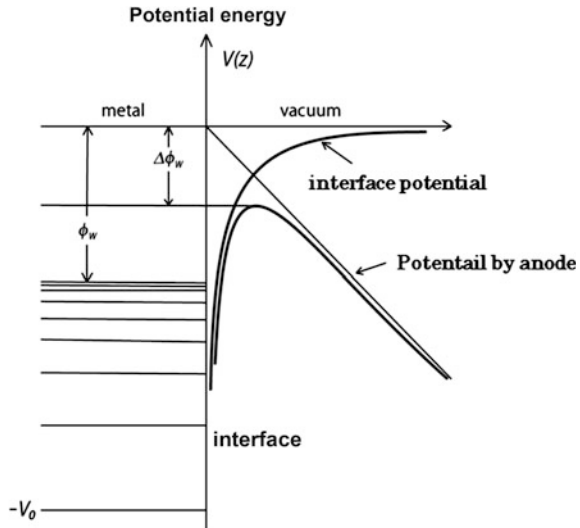


$$i = A' F^2 \exp(-B' \phi_w / F) \quad (2.3)$$

where  $\phi_w$  is the work function for metals,  $F$  is the field strength near the tip, and  $A'$  and  $B'$  are constants. This is the famous Fowler and Nordheim equation (Liboff 2003). The brightness of the FEG is larger than  $10^8$  A/cm<sup>2</sup>sr. The FEG has two modes for temperature of the tip: the cold-field emission gun (c-FEG) and the thermal-field emission gun (t-FEG). In the latter, the temperature of the cathode is around 1300 K, lower than that of the thermionic gun. The gun uses a region between the thermionic emission ruled by Eq. (2.2) and the electron tunneling ruled by Eq. (2.3).

To obtain a sufficient brightness from the c-FEG, an extraction anode and a succeeding accelerating electrode should be optimized. One design is use of two

**Fig. 2.3** Energy level diagram of a metal/vacuum interface with an electrostatic potential by an anode in an electron gun



quadratic curves in the space between the two anodes, which was theoretically proposed by Butler (1966), as illustrated in Fig. 2.2b. Another curve of a simple funnel shape was studied by Tonomura (1973). The thermal field emission gun has an advantage of the large total current and usability without ultra high vacuum inside the gun. Recent analytical TEM uses FEGs for a probe with higher electron intensity.

The coherence characteristics which determine interference phenomena between two waves is determined by electron guns. The temporal coherence is determined by fluctuations of accelerating voltage ( $E$ ) and that of the Fermi velocity of electrons inside the cathode materials. The spatial coherence is determined by the size of the cathode and design of the arrangement of the gun, condenser lens, and a specimen. The issue shall be discussed in Chap. 7.

### Electron lens

Next, we move on to the lens for electrons. There are two kinds of lenses such as an electrostatic lens and an electromagnetic lens. The former is used in the Wehnelt electrode for making a crossover of electrons below the electron gun in modern TEM instruments.

In this section, we focus on a magnetic lens for imaging such as an objective lens. For the invention of electron microscopes, it was essentially important that the axial symmetrical magnetic field was discovered to work as a convex lens for electrons with a negative charge. Since the beginning of the 1920s, various studies for increasing intensity of bright spots in a cathode-ray oscillograph (=oscilloscope) were performed in the Berlin Institute of Technology (Busch et al. 1927).

The magnetic lens has several types, which are axially symmetric and non-symmetric along the optical axis. The latter named “pole lens” is recently limelighted for aberration correction and shall be explained in Chap. 8. Hereafter, we study an axial symmetric magnetic lens named as round lens.

The lenses after the electron source in TEM are a condenser lens, an objective lens, an intermediate lens, and a projector lens.

The condenser lens works for illuminating specimens with slightly focusing electrons from the source. In TEM, particularly, the “Koeller illumination mode” is used, where the lens works for making a parallel beam along the optical axis for a specimen. In a sense of wave optics, the incident wave is considered as a plane wave. For HRTEM, brighter illumination is crucial. The condenser lens is more excited to focus the electron beam onto the specimen, and this is named as “critical illumination.” In this case, a kind of converging beam is realized, whose inclination angle determines the spatial coherence (see Sect. 7.3.3).

The objective lens is a most important lens, because it faces directly a specimen and works as the imaging lens. The mechanism of the objective lens for electrons is described in later section. At the moment, we notice that the famous lens formula such as  $1/a + 1/b = 1/f$  holds in the imaging theory of TEM. The typical magnification for enlargement is around 50–100.

The next intermediate lens is a unique lens which does not exit in an optical microscope. It works for the change of magnification and for the change of imaging/diffraction modes. A slight change of the lens excitation introduces the change of magnification of TEM. A large change gives the change of imaging/diffraction modes because the focus point of the lens is moved from the image plane of the objective lens to the diffraction plane.

The final lens for imaging is the projector lens, which works for the enlargement of images and diffraction patterns. The images and patterns in outer areas are always deformed by off-axis aberrations, which are corrected after recording using a standard specimen such as a silicon crystal or a grating.

## 2.2 Basic Action of a Magnetic Round Lens

The action of the magnetic lens is based on Newton’s equation with the Lorentz force of charged particles  $q$  ( $= -e$ ) in a magnetic field  $\mathbf{B}$  as follows,

$$m \frac{d^2 \mathbf{r}}{dt^2} = (-e) \mathbf{v} \times \mathbf{B}, \quad (2.4)$$

where  $\mathbf{r}$  is a positional vector of an electron,  $\mathbf{v}$  is a velocity vector, and  $\mathbf{B}$  is a magnetic field (magnetic induction). We can assume the axial symmetry along the optical axis. The electron runs spirally as well as moves along the axis ( $z$ -axis). The interaction part of lens action is a radial component of the differential Eq. (2.4). The radial function of positions of the electron as a function of  $R(r)$  determines a focusing characteristic of the lens (see Hawkes and Kasper 1989).

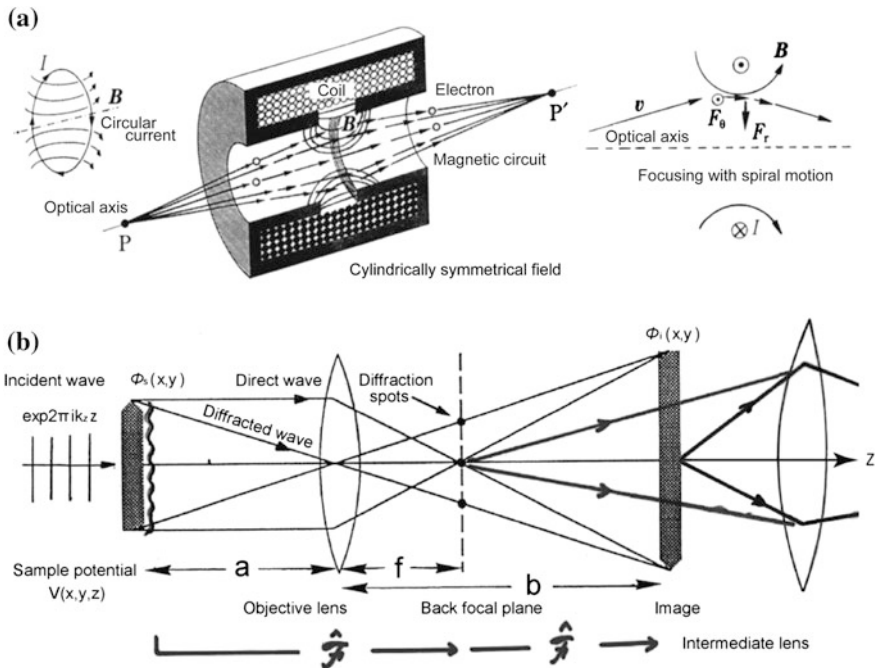


**Fig. 2.4** Basic structure and mechanism of an electromagnetic lens for electrons (a) and ray diagram for imaging by a convex lens and its action expressed in terms of two times of Fourier transform (b)

Before explanation using mathematical formula, we try to understand the action of the magnetic lens using illustrations. Figure 2.4a shows a convex lens for electrons, which is composed of coils with the turning axis parallel with the optical axis. The magnetic field caused by the coils is a multiple addition of the magnetic field caused by a circle current as illustrated in the left-hand side of Fig. 2.4a. Additionally, a yoke of a soft iron encloses the coils, which confines the magnetic field in the yoke to strengthen the field in a gap (see a black box). We set a pole-piece made of another iron-alloy (= “permendur”) at the gap. This gap gives the action of a convex lens. The quality of manufacturing of the pole piece determines the final performance of the magnetic lens, whose irregularity produces a kind of aberration named the “parasitic aberration.”

The magnetic field caused by the coils works as a convex lens, where a charged particle emitted from a point in the optical axis is focused on the opposite side of the coils, as shown in the center of Fig. 2.4a. This is the basis of the imaging by a convex lens for electrons. The particles emitted from a point a little off the optical axis are focused by the magnetic field, but do not make a point. This corresponds to a blurred image and in other word, off-axial aberration (see Sect. 8.4.2). In electron optics, we can trace an electron trajectory (ray path) emitted from an object near optical axis. This treatment is named the “paraxial approximation” in optics. We

can only care for angular distribution of electrons from the object in optical axis (see Born and Wolf 1970).

Next, we try to understand why the electrons are focused by the axially symmetrical magnetic field. In a figure in the right-hand side of Fig. 2.4a, an electron with  $v$  enters the magnetic field denoted by an arc and receives the Lorentz force in a direction from backside to front side of a paper of this book. The electron starts with rotation and then receives an additional force down side by the Lorentz force, which is caused between a bended velocity and the magnetic field. As a result, the electron has rotation and focusing in a form of a shrinking spiral form along the optical axis.

This focusing action occurs for electrons emitted from a paraxial point near the optical axis, and they are focused on another paraxial point in the opposite side of the lens for forming a reversed image.

For high-energy electrons such as 200 keV, the wavelength is 0.0028 nm. The diffraction/scattering angle by 200 lattice planes of gold ( $d = 0.21$  nm) is 0.013 rad ( $\alpha = \lambda/d = 0.0028 \text{ nm}/0.21 \text{ nm}$ ) or  $0.74^\circ$ , which is a very small angle!

Also for high-resolution electron microscopy, the size of observing areas is about several tens of nanometer. From the viewpoint of lateral positions of the electron trajectory and its angular distribution, the “paraxial approximation” holds with a good accuracy. The aberration such as blurring of images can be treated using the power series of diffraction/scattering angle  $\alpha$  in the approximation. In the exact theory of aberration, we use complex variables  $\omega$  for describing the scattering angle  $\alpha$  including rotational angle around the optical axis  $\phi$  (see Chap. 18).

## 2.3 Mathematics for Describing Lens Actions

To describe the motion of electrons in the magnetic field, we use the cylindrical coordinates  $(r, \phi, z)$  in Newton’s equation of motion.<sup>3</sup> The motion related to  $\phi$  is a rotation motion around the optical axis, as illustrated in Fig. 2.5.

Setting the axially symmetrical magnetic field  $(B_r, B_\phi, B_z)$ , the motion of electrons is described by classical mechanics and Lorentz force (see Eq. (2.4)). From the viewpoint of symmetry of the field,  $B_\theta = 0$ , then we have equations of motion using other components such as  $B_r, B_z$

$$m(\ddot{r} - r\dot{\phi}^2) = -e\dot{\phi}B_z \quad (2.5)$$

---

<sup>3</sup>The fact that the motion of electrons in the field much larger than atomic size can be treated by classical mechanics, not quantum mechanics, can be understood though studying the WKB approximation in textbooks of quantum mechanics (see Schiff 1968; Bohm 1951). This is similar to the transition of geometrical optics to wave optics by using a physical quantity as “eikonal” (see Born and Wolf 1970 and Chap. 29).



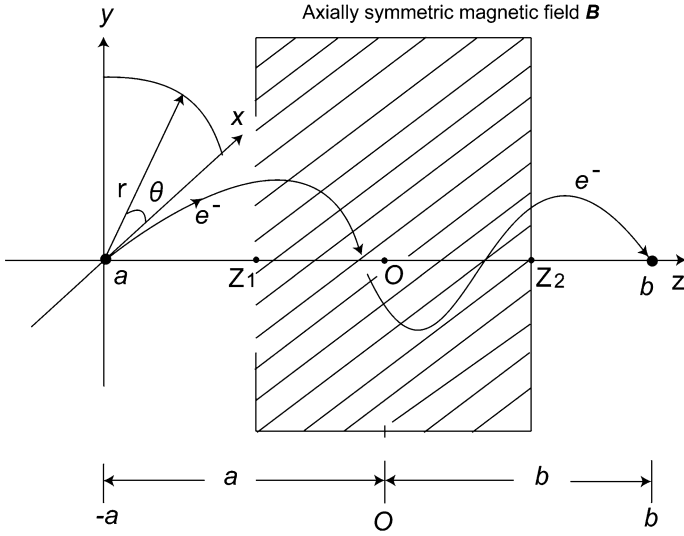


**Fig. 2.5** Trajectory of an electron in the electron magnetic lens with rotation and focusing along an optical axis ( $z$ -axis)

$$m \frac{1}{r} \frac{d}{dt} (r^2 \dot{\phi}) = -e(v_z B_r - v_r B_z), \quad (2.6)$$

where the dot in the above symbols shows time-differential operation.

Changing  $B_z$  into a magnetic field  $B(z)$  at  $r = 0$ , and assuming that  $r \cong 0$  for the trajectory of electrons (= paraxial approximation), we have  $\dot{\phi} = \frac{e}{2m} B(z)$ . Then, with  $v_z = \sqrt{\frac{2eE}{m}}$ , the integration becomes  $\phi = \sqrt{\frac{e}{8me}} \int_{z_1}^{z_2} B(z) dz$ . The electrons have the spiral motion of electrons produced in the magnetic field in the area of  $z_1 \sim z_2$ , as shown in Fig. 2.5. It is noted that microscopic images are enlarged with rotation.<sup>4</sup>

To separate the  $r$ -component and  $\phi$ -one of the equation, we can also use Lamor's coordinate system, where the axes of cartesian coordinates of  $x$  and  $y$  are rotated with the lamor frequency  $\omega_L$  in the optical axis (see Hawkes and Kasper 1989). The transformations are as follows:

$$X = x \cos \omega_L t - y \sin \omega_L t \quad (2.7)$$

$$Y = x \sin \omega_L t + y \cos \omega_L t \quad (2.8)$$

$$\left( \omega_L = \frac{eB(z)}{2m} \right)$$

<sup>4</sup>In modern TEM, the rotation, which is inconvenient for actual observation and recording, is minimized in the image and diffraction planes by a combination of many convex lenses.

Next, we consider the motion in the direction of  $r$ . Using  $v_\phi = r\dot{\phi}$  and Eq. (2.5), we have the differential equation as  $\ddot{r} = -\frac{e^2[B(z)]^2}{4m^2}r$ . Using  $\frac{d}{dt} = \sqrt{\frac{2eE}{m}}\frac{d}{dz}$ , which uses the approximate form of Eq. (1.3), we have

$$\frac{d^2r}{dz^2} + \frac{e[B(z)]^2}{8mE}r = 0 \quad (2.9)$$

The equation determines the distance of the electron trajectory from the optical axis and the focal length of the convex lens.

Now, we formulate the focal length. Although electrons make the spiral motion along the optical axis from point  $A(z = -a)$  in the object space and a point  $B(z = b)$  in the image space, we need to only consider the variation of  $r$  from the integration in Eq. (2.9) as

$$\left(\frac{dr}{dz}\right)_b - \left(\frac{dr}{dz}\right)_{-a} = -\frac{e}{8mE} \int_{-a}^b r[B(z)]^2 dz \quad (2.10)$$

When the thickness of the magnetic field is small ( $z_1 < z < z_2$ ), the distance from the optical axis is not so much changed. This is named the “approximation of thin lens.” Setting  $r(z) = r_l$  in an area of  $z_1 \sim z_2$

$$a\left(\frac{dr}{dz}\right)_{-a} = -b\left(\frac{dr}{dz}\right)_b \quad (2.11)$$

The equation can be derived from the fact that the gradient of the trajectory at a point A is determined by  $r_l/a$ .

$$\frac{1}{b} + \frac{1}{a} = \frac{e}{8mE} \int_{-a}^b [B(z)]^2 dz = \frac{e}{8mE} \int_{z_1}^{z_2} [B(z)]^2 dz \quad (2.12)$$

Setting ( $-a \rightarrow -\infty$ ), the point with  $b$  becomes the focal point, and then we have the following equation of the focal length.

$$\frac{1}{f} = \frac{e}{8mE} \int_{z_1}^{z_2} [B(z)]^2 dz \quad (2.13)$$

The equations of (2.12) are the same as that of thin optical lens, as illustrated in Fig. 2.4b. However, for strongly excited magnetic lenses, we have to use the formulation of “thick lens” in optics (see Born and Wolf 1970; Hawkes and Kasper 1989). From the Eqs. (2.5) and (2.6), it is understood that the rotation angle and the focal length are determined by the  $z$ -component of the magnetic field  $B$ .

The distribution  $B(z)$  is accurately obtained by solving the equation using a magnetostatic potential determined by the shape of the pole-piece using the finite element method (FEM).

In actual calculations, the following bell-shaped potential is useful for most of the practical design.

$$B(z) = \frac{B_0}{1 + \left(\frac{z}{a}\right)^2}, \quad (2.14)$$

where  $a$  is the width and  $B(z)$  is  $0.5B_0$ .

Using these equations and theories of geometrical aberrations, we can discuss the spherical and chromatic aberrations which are very important for high-resolution electron microscopy. The reader should refer to the Chap. 18 in the present book and consult with another technical book (Hawkes and Kasper 1989).

## 2.4 Summary

- (1) We study the structures of a transmission electron microscope in analogy of an optical microscope, although the physical principle of the components is different from those of optical microscope. The arrangement of the parts is similar and understood on the basis of wave optics, whose basis is Fourier transform.
- (2) The source of electrons has various kinds such as a thermionic cathode, thermal or cold FEGs, and a photocathode.
- (3) A convex lens is composed of an axially symmetrical magnetic field produced by electrical coils covered by a yoke of a soft iron and a pole piece with a special iron–cobalt alloy named “permendur.”
- (4) The motion of an electron in a convex lens can be treated by classical mechanics using Newton’s equation, while the Schrodinger equation is not necessary. Electrons running near the optical axis converge by Lorentz force with the Larmor rotation, which introduces the rotation of images and diffraction patterns in TEM.

## Problems

- 2.1 Derive the lens formula of thin lens in light optics by yourself. See textbooks in high school.
- 2.2 Derive the Eqs. (2.5) and (2.6) from Newton’s equation of motion in cylindrical coordinates.
- 2.3 Study “Lamor coordinates” by seeing the internet or Hawkes and Kasper’s book.

## References

- Bohm, D. (1951). *Quantum theory*. New York: Prentice Hall.
- Born, M., & Wolf, E. (1970). *Principles of optics*. Oxford: Pergamon Press.
- Broers, A. N. (1967). *Journal of Applied Physics*, 38, 1991.
- Busch, H. (1927). *Architecture Electrotechnology*, 18, 583.
- Butler, J. W. (1966). In R. Uyeda (Ed.), *Sixth international. Congress on Electron Microscopy*. Maruzen, Tokyo.
- Hawkes, P. W., & Kasper, E. (1989). *Principles of electron optics*. London: Academic Press.
- Hibi, T. (1956). *Journal of Electron Microscopy*, 4, 10.
- Kittel, C. (1966). *Introduction to solid state physics*. New York: John Wuley & Sons Inc.
- Liboff, R. L. (2003). *Introductory quantum mechnics*. San Franscisco: Addison Wesley.
- Schiff, L. I. (1968). *Quantum mechnaics*. New York: McGraw-Hill.
- Seidel, L. (1856). *Astronomische Nachrichten*, 43, 289.
- Tonomura, A. (1973). *Japanese Journal of Applied Physics*, 12, 1065.

Electron Nano-Imaging

Basics of Imaging and Diffraction for TEM and STEM

Tanaka, N.

2017, XXVIII, 333 p. 129 illus., 22 illus. in color.,

Hardcover

ISBN: 978-4-431-56500-0